Chinese Physics Letters **40**, 014301 (2023)

Superscattering of Underwater Sound via Deep Learning Approach

Wenjie Miao(缪文杰), Zhiang Linghu(令狐志盎), Qiujiao Du(杜秋姣),
Pai Peng(澎湃), and Fengming Liu(刘丰铭)*

School of Mathematics and Physics, China University of Geosciences, Wuhan 430074, China

(Received 29 October 2022; accepted manuscript online 7 December 2022)

We design a multilayer cylindrical structure to realize superscattering of underwater sound. Because of the near degeneracy of resonances in multiple channels of the structure, the scattering contributions from these resonances can overlap to break the single-channel limit of subwavelength objects. However, tuning the design parameters to achieve the target response is an optimization process that is tedious and time-consuming. Here, we demonstrate that a well-trained tandem neural network can deal with this problem efficiently, which can not only forwardly predict the scattering spectra of the multilayer structure with high precision, but also inversely design the required structural parameters efficiently.

DOI: 10.1088/0256-307X/40/1/014301

Acoustic metamaterials (AMs) have become a very hot research topic across disciplines due to their many potentially revolutionary applications over the past decades.[1–5] AMs derive their novel abilities from the interaction between sound and various kinds of constituent units. These constituent units are commonly on a subwavelength scale, which permits their effective parameters to take extreme values. Therefore, understanding the scattering characteristics of individual constituent unit is scientifically and practically important for research of AMs. Strength of scattering is characterized by the absolute or area-normalized scattering cross section (SCS). In terms of the absolute SCS, one can prove that the maximum SCS of a subwavelength scatterer is constrained in two dimensions (2D) and in three dimensions (3D), which is referred as the single-channel limit.[6,7] Although some applications of AMs, for example, acoustic cloaking,[8–11] require SCS as small as possible, strong enhancement of scattering is important for other applications, such as acoustic antennas and acoustic sensing.[12–17] Recently, we have designed a solid maze-like rod to achieve airborne sound superscattering effect.[18] However, the maze-like structure requires a large impedance mismatch between air and solid to provide highly reflective boundaries for airborne sound, which is impossible for solid structures in water. Therefore, an acoustic meta-atom with a feasible structural design is still needed to achieve underwater sound superscattering.

Inspired by the previous studies on the superscattering effect of light,[19] we search for similar structures that can support low-frequency resonance in water. Note that a soft enough solid structure, such as a rubber rod, can support low-frequency resonance to achieve strong scattering in the deep-subwavelength regime. However, it is difficult for too soft materials to maintain their shape in water. Therefore, we propose multilayer cylindrical structures composed of soft and hard solids, which can not only achieve sub-wavelength strong scattering but also maintain its shape in water. The multilayer structures provide designable parameters and are hence highly tunable to realize a diverse spectrum. However, the relation between design parameters and sound response is quite complicated, and tuning the design parameters to achieve the target response is very time-consuming. Indeed, it would be highly desirable if the design problem can be solved as an inverse scattering problem.

The rapid development of deep learning techniques has enabled researchers to efficiently solve numerous physical problems, such as optimization of photonic structures,[20,21] high-resolution imaging,[22,23] and broadband acoustic cloak.[24] Notably, compared to traditional methods such as genetic algorithms, neural networks are particularly efficient in solving difficult inverse problems in design complex structures for different applications. The inverse design process allows for fast and accurate prediction of the design parameters. In this work, we demonstrate that an artificial network can be used to inversely design multilayer cylindrical structures for superscattering of underwater sound in the desired frequency range. We note that a variety of networks that can generate probabilistic geometric parameters have been used to calculate a multitude of physical responses.[25] However, most of them require strong computational power, consume time, and have high relative errors. Thus, we use the method of tandem neural network (TNN). It can overcome the biggest problem in the inverse design: one-to-many mapping.[26] We first establish and train a forward neural network (FNN) which maps the design parameters to the spectral response, and then build a tandem neural network by connecting it with the inverse network. After the training process, our tandem network is involved to give a set of design parameters to match the targeted spectrum. In addition, we perform full-wave simulations to verify the predicted acoustic superscattering effects.

A 2D multilayer cylindrical structure is proposed to realize the sound superscattering effect. The multilayer cylinder is composed of a Fe ($\rho_{\rm Fe} = 7670\,{\rm kg/m^3}$, $c_{\rm lFe} = 6010\,{\rm m/s}$, $c_{\rm tFe} = 3230\,{\rm m/s}$) core and four alternating shells of rubber ($\rho_{\rm Rubber} = 1160\,{\rm kg/m^3}$, $c_{\rm lRubber} = 490\,{\rm m/s}$,

*Corresponding author. Email: liufm@cug.edu.cn
© 2023 Chinese Physical Society and IOP Publishing Ltd

$c_{\text{tRubber}} = 240\,\text{m/s}$) and PMMA ($\rho_{\text{PMMA}} = 1200\,\text{kg/m}^3$, $c_{\text{lPMMA}} = 2830\,\text{m/s}$, $c_{\text{tPMMA}} = 1160\,\text{m/s}$), as illustrated in Fig. 1(a). We note that a similar multilayer cylinder has been designed to achieve acoustic cloaking via deep learning approach.[27] In that work, only different fluid materials were considered to compose the multilayer cylinder. It is clear that our solid structure is more practicable in a fluid background. As the constituent materials have been determined, the properties of our multilayer cylindrical structure are described by its radius r, and the mth layer of the structure is characterized by its outer radius r_m, where $m = 1, 2, 3, 4, 5$ is the layer index. In order to analyze the scattering response of the structure, the Mie scattering theory has been used to generate the training data samples, where we determine the SCS spectra for random radius space, $R = [r_1, r_2, r_3, r_4, r_5]$. The spectrum is divided to 100 discrete points covering the normalized frequency range, with a equal to the outer radius r_5. Each training sample is represented by five geometric parameters and 100 discrete points of SCS spectrum $S = [s_1, s_2, s_3, s_4, \ldots, s_{100}]$. We design the FNN that maps the design R to the spectrum S, and the inverse neural network that maps the spectrum S to the design R. In the inverse design, we use a TNN to solve the problem of non-uniqueness of the solutions. Both the forward and inverse networks are trained by optimizing the neural network weights. It is worth noting that the inverse training does not change the weights of the forward network. To build the database, we generate 100000 data samples for random parameters, which are divided into two different groups: 95000 data samples for the training and 5000 data samples for the validation. The training data are used to train the network by optimizing the neural network weights, and the validation data are used to check the correctness and accuracy of the network prediction. As an example, Fig. 1(b) shows absolute SCSs for a multilayer superscatterer. It can be seen that a resonant peak appears in the SCS spectrum of the superscatterer, and its value is approximately four times the value of the single-channel limit. As the superscatterer has a deep-subwavelength radius of 0.135λ, a superscattering effect is indeed achieved. For comparison, the SCSs of homogeneous PMMA and Fe cylinders are also presented in Fig. 1(b). The PMMA and Fe cylinders have radii which are the same as the outer radius of the superscatterer. It can be expected that such tiny homogeneous cylinders will hardly scatter acoustic waves in the subwavelength regime.

Forward Neural Network. We first design the FNN to accurately predict the SCS spectrum as a function of frequency for given parameters. The forward model takes the geometric structure R as the input and the SCS spectrum as the output layer of the FNN, as shown in Fig. 1(c). The data are normalized before training to accelerate the convergence speed of the network. During the training process, the training data are fed into the network and its weights W are continuously optimized to minimize the loss function described as $L = \frac{1}{N}\sum_k |s_k - \hat{s}_k|$, where s_k and $\hat{s}_k$ are the actual spectrum and the spectrum predicted by the neural network, respectively. The FNN is optimized with six fully connected layers with each layer having 100–300–400–500–400–100 neurons, respectively. The remaining hyperparameters (batch size, learning rate, activation function, etc.) are judiciously selected to minimize the loss function in the validation set. The learning curves of the loss functions of the training and validation data as a function of epoch are shown in Fig. 2(a). As the training proceeds, both the training set error and the validation set error decrease, until they converge after 200 iterations, implying the completion of the training phase. To check the prediction accuracy of the trained model, 5000 data samples of validation set are used to evaluated it. The predicted results of the trained network are compared with the results obtained by the Mie scattering theory, and the loss function value of the validation set is 0.0035, which proves the high prediction accuracy of the network. Figures 2(b)–2(d) show the spectra of three representative samples obtained by the FNN, the Mie scattering theory and the finite element method (COMSOL MULTIPHYSICS). All the results obtained in the three different ways coincide perfectly. As an example, we draw the scattered pressure fields from individual channel in Fig. 2(c), which shows that the main contributions to the total SCS come from the near degeneracy of the monopole and dipole modes. We also perform full-wave numerical simulations to better demonstrate the superscattering effect. Figures 3(a)–3(c) display the total pressure-field distribution at the normalized frequency $ka = 0.5$, when plane waves illuminate the superscatterer, homogeneous PMMA and Fe cylinders, respectively, from the left side. The total pressure-field distribution exhibits a significant "shadow" behind the superscatterer, and the size of the shadow is much larger than the size of the superscatterer due to the superscattering effect. Meanwhile, for the PMMA and Fe cylinders with the same sizes as the superscatterer the incident plane waves are hardly disturbed by these tiny homogeneous cylinders.

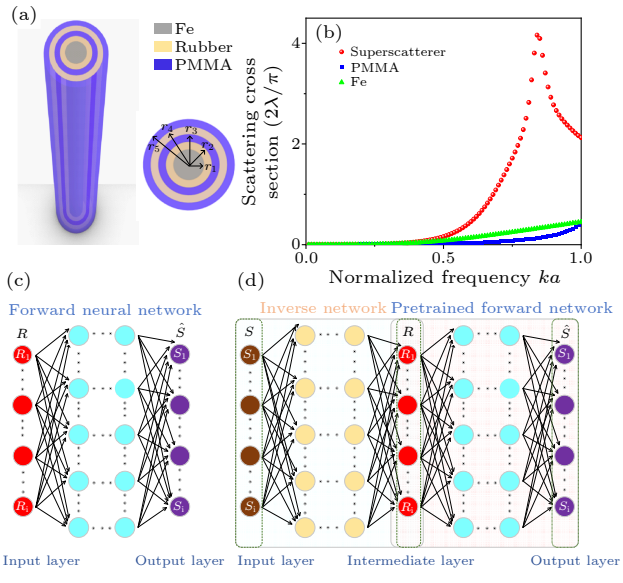

Fig. 1. (a) Schematic illustration of a multilayer cylindrical structures. (b) Absolute SCSs for a multilayer superscatterer, and for PMMA and Fe cylinders. The PMMA and Fe cylinders have the same radius as the outer radius of the superscatterer. (c) Forward neural network, S is the spectral response, R is the geometry parameters. (d) Proposed tandem network model for forward prediction and inverse design, S is the spectral response, and R is the geometry parameters.

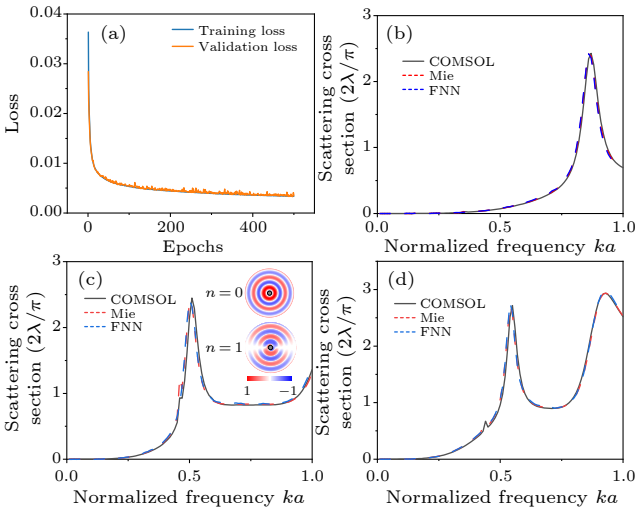

Fig. 2. (a) Learning curves for training and validation sets as a function of training epochs. (b)–(d) Comparison of the SCS spectra of three representative samples obtained by the FNN, Mie scattering theory, and COMSOL. Scattered pressure fields from individual channel with $n = 0$ and $n = 1$ are also plotted in (c).

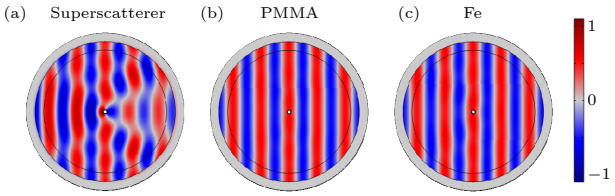

Fig. 3. Numerical total pressure-field distribution produced by incident plane waves for (a) the superscatterer, (b) the homogeneous PMMA cylinder, (c) the homogeneous Fe cylinder. The normalized frequency $ka = 0.5$ is picked from the spectral response shown in Fig. 2(c).

Tandem Neural Network. In the practical application of metamaterials, various parameters often need to be designed to obtain the desired spectral response, which is usually time-consuming and inefficient. Here, we require a tool to significantly reduce the computational time for the accurate inverse design of superscattering structures. To achieve this goal, we use a TNN, where the inverse neural network is tandemly connected to the pre-trained forward modeling network, as shown in Fig. 1(d). The pre-trained forward network substitutes the Mie theory calculation and acts as a data generator in the training. Compared with the Mie theory calculation, the pre-trained forward network has a faster computing time, while maintaining a good prediction accuracy for the designed spectral response. In the inverse training process, the pre-trained forward network has fixed weights and bias, while the weights of the inverse network are updated by minimizing the loss function of the inverse neural network. The designed structure refers to intermediate layers R in the TNN that predicts the five design parameters for the desired spectral response. The structure of the inverse network is designed to have seven fully connected layers with each layer composed of 200–500–600–300–200–100–5 neurons, respectively. We use 5000 validation data to examine the accuracy of the inverse neural network just like in the forward network. We randomly select target spectra from the sampling data that have never been used in the previous training, so that the target spectra are physically realizable. As shown in Fig. 4(a), the loss function learning curves for the training and validation loss decrease rapidly and the loss function drops to 0.0345 after 1500 epochs of training. Through the inverse design, the network finds out the correct design parameters. Figures 4(b)–4(d) depict the spectral response for three representative samples. The spectra predicted by the inverse neural network shows good agreement with target input spectra calculated by the Mie theory. We can also use the finite element method to calculate the spectra since the design parameters have been obtained. The perfect agreement between these results confirms the effectiveness of our neural network in inverse design.

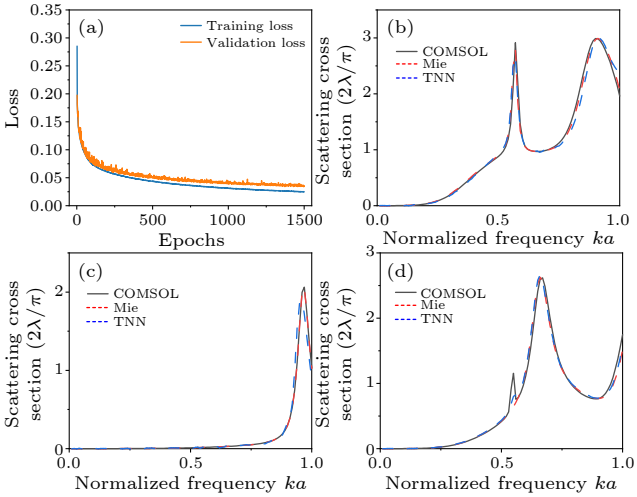

Fig. 4. (a) Learning curves for training and validation sets as a function of training epochs. (b)–(d) Three representative samples using the TNN to design the structure. The red dashed lines are the target spectra. The blue dashed lines represent the spectra predicted by the TNN. The black solid lines represent the results calculated by COMSOL.

In summary, we have propose a deep-learning-assisted method to achieve hybrid multilayer structure for superscattering of underwater sound. We firstly show that an FNN can predict the scattering spectra of the proposed superscatterer with high precision. Then, a TNN has been utilized to solve inverse design problems. After the training, the TNN can solve one-to-many problems and give the corresponding design parameters for target scattering spectra effectively and efficiently. We expect that our approach can be easily applied to the inverse design of various practical acoustic applications.

Acknowledgement. This work was supported by the National Natural Science Foundation of China (Grant Nos. 12174353, 41974059, and 41830537).

References

[1] Liu Z Y, Zhang X X, Mao Y W, Zhu Y Y, Yang Z Y, Chan C T, and Sheng P 2000 *Science* **289** 1734

[2] Pendry J B, Schurig D, and Smith D R 2006 *Science* **312** 1780

[3] Cummer S A, Christensen J, and Alu A 2016 *Nat. Rev. Mater.* **1** 16001
[4] Ma G C and Sheng P 2016 *Sci. Adv.* **2** e1501595
[5] Assouar B, Liang B, Wu Y, Li Y, Cheng J C, and Jing Y 2018 *Nat. Rev. Mater.* **3** 460
[6] Aizpurua J, Hanarp P, Sutherland D S, Kall M, Bryant G W, F J, and de Abajo G 2003 *Phys. Rev. Lett.* **90** 057401
[7] Tribelsky M I and Lykyanchuk B S 2006 *Phys. Rev. Lett.* **97** 263902
[8] Leonhardt U 2006 *Science* **312** 1777
[9] Schurig D, Mock J J, Justice B J, Cummer S A, Pendry J B, Starr A F, and Smith D R 2006 *Science* **314** 977
[10] Zhu X F, Liang B, Kan W W, Zou X Y, and Cheng J S 2011 *Phys. Rev. Lett.* **106** 014301
[11] Zhang S, Xia C G, and Fang N 2011 *Phys. Rev. Lett.* **106** 024301
[12] Chen Y Y, Liu H J, Reilly M, Bae H, and Yu M 2014 *Nat. Commun.* **5** 5247
[13] Fleury R, Sounas D, and Alu A 2015 *Nat. Commun.* **6** 5905
[14] Lu G X, Ding E L, Wang Y Y, Ping X Y, Cui J, Liu X Z, and Liu X J 2017 *Appl. Phys. Lett.* **110** 123507
[15] Bogue R 2017 *Sens. Rev.* **37** 305
[16] Fan X D, Zhu Y F, Liang B, Cheng J C, and Zhang L K 2018 *Phys. Rev. Appl.* **9** 034035
[17] Landi M, Zhao J J, Prather W E, Wu Y, and Zhang L K 2018 *Phys. Rev. Lett.* **120** 114301
[18] Liu F M, Zhang S, Luo L C, Li W P, Wang Z Y, and Ke M Z 2019 *Phys. Rev. Appl.* **12** 064063
[19] Luo J, Li X, Zhang X Y, Guo J J, Liu W, Lai Y, Zhan Y H, and Huang M 2021 *Opt. Express* **29** 10527
[20] Peurifoy J, Shen Y C, Jing L, Yang Y, Cano-Renteria F, DeLacy B G, Joannopoulos J D, Tegmark M, and Soljacic M 2018 *Sci. Adv.* **4** eaar4206
[21] So S, Mun J, and Rho J 2019 *ACS Appl. Mater. Interfaces* **11** 24264
[22] Liu Q S, Hang R L, Song H H, and Li Z 2018 *IEEE Trans. Geosci. Remote Sens.* **56** 117
[23] Orazbayev B and Fleury R 2020 *Phys. Rev. X* **10** 031029
[24] Qian C, Zheng B, Shen Y C, Jing L, Li E P, Shen L, and Chen H S 2020 *Nat. Photon.* **14** 383
[25] Luo Y T, Li P Q, Li D T, Peng Y G, Geng Z G, Xie S H, Li Y, Alu A, Zhu J, and Zhu X F 2020 *Research* **2020** 8757403
[26] Liu D J, Tan Y X, Khoram E F, and Yu Z F 2018 *ACS Photon.* **5** 1365
[27] Ahmed W W, Farhat M, Zhang X L, and Wu Y 2021 *Phys. Rev. Res.* **3** 013142